

TOPOLOGICAL OPTIMIZATION OF STRUCTURES SUBJECT TO VON MISES STRESS CONSTRAINTS

S. AMSTUTZ AND A.A. NOVOTNY

ABSTRACT. The topological asymptotic analysis provides the sensitivity of a given shape functional with respect to an infinitesimal domain perturbation. Therefore, this sensitivity can be naturally used as a descent direction in a structural topology design problem. However, according to the literature concerning the topological derivative, only the classical approach based on flexibility minimization for a given amount of material, without control on the stress level supported by the structural device, has been considered. Yet, one of the most important requirements in mechanical design is to find the lightest topology satisfying a material failure criterion. In this paper, therefore, we introduce a class of penalty functionals that mimic a pointwise constraint on the Von Mises stress field. The associated topological derivative is obtained for plane stress linear elasticity. Only the formal asymptotic expansion procedure is presented, but full justifications can be easily deduced from existing works. Then, a topology optimization algorithm based on these concepts is proposed, that allows for treating local stress criteria. Finally, this feature is shown through some numerical examples.

1. INTRODUCTION

Structural topology optimization is an expanding research field of computational mechanics which has been growing very rapidly in the last years. For a survey on topology optimization methods, the reader may refer to the review paper [17], or to the monographs [2, 11, 23]. A relatively new approach for this kind of problem is based on the concept of topological derivative [15, 18, 33]. This derivative allows to quantify the sensitivity of a given shape functional with respect to an infinitesimal topological domain perturbation, like typically the nucleation of a hole. Thus, the topological derivative has been successfully applied in the context of topology optimization [7, 13, 28], inverse problems [5, 12, 20, 29] and image processing [9, 25, 24, 26]. Concerning the theoretical development of the topological asymptotic analysis, the reader may refer to [30], for instance. However, in the context of structural topology design, the topological derivative has been used as a descent direction only for the classical approach based on minimizing flexibility for a given amount of material. Although widely adopted, through this formulation the stress level supported by the structural device cannot be controlled. This limitation is not admissible in several applications, because one of the most important requirements in mechanical design is to find the lightest topology satisfying a material failure criterion. Even the methods based on relaxed formulations [1, 10, 11] have been traditionally applied to minimum compliance problems. In fact, only a few works dealing with local stress control can be found in the literature (see, for instance, [3, 4, 14, 16, 19, 31]). This can be explained by the mathematical and numerical difficulties introduced by the large number of highly non-linear constraints associated to local stress criteria.

Following the original ideas presented in [8] for the Laplace equation, in this paper we introduce a class of penalty functionals in order to approximate a pointwise constraint on the Von Mises stress field. The associated topological derivative is then obtained for plane stress linear elasticity. We show that the obtained topological asymptotic expansion can be used within a topology optimization algorithm, which allows for treating local stress criteria. Finally, the efficiency of this algorithm is verified through some numerical examples. In particular, the obtained structures are free of geometrical singularity, unlike what occurs by the compliance minimization

Key words and phrases. topological sensitivity, topological derivative, topology optimization, local stress criteria, von Mises stress.

approach. We recall that such singularities lead to stress concentrations which are highly undesirable in structural design. For a detailed description of the stress concentration phenomenon, the reader may refer to [22, 32].

The paper is organized as follows. The plane stress linear elasticity problem and the proposed class of Von Mises stress penalty functionals are presented in Section 2. The topological derivative associated to these functionals is calculated in Section 3. The proposed topology design algorithm is described in Section 4. Finally, Section 5 is dedicated to the numerical experiments.

2. PROBLEM STATEMENT

In this Section we introduce a class of Von Mises stress penalty functionals under plane stress linear elasticity assumptions.

2.1. The constrained topology optimization problem. Let D be a bounded domain of \mathbb{R}^2 with Lipschitz boundary Γ . We assume that Γ is split into three disjoint parts Γ_D , Γ_N and Γ_0 , where Γ_D is of nonzero measure, and Γ_N is of class C^1 . We consider the topology optimization problem:

$$\text{Minimize } I_\Omega(u_\Omega) \quad (2.1)$$

$\Omega \subset D$

subject to the state equations

$$\begin{cases} -\text{div}(\gamma_\Omega \sigma(u_\Omega)) = 0 & \text{in } D, \\ u_\Omega = 0 & \text{on } \Gamma_D, \\ \gamma_\Omega \sigma(u_\Omega) n = g & \text{on } \Gamma_N, \\ \sigma(u_\Omega) n = 0 & \text{on } \Gamma_0, \end{cases} \quad (2.2)$$

and the constraint

$$\sigma_M(u_\Omega) \leq \bar{\sigma}_M \quad \text{a.e. in } \Omega \cap \tilde{D}. \quad (2.3)$$

The notations used above are the following. The system (2.2) is understood in the weak sense, as this will be the case throughout all the paper, and admits an unique solution

$$u_\Omega \in \mathcal{V} = \{u \in H^1(D)^2, u|_{\Gamma_D} = 0\}.$$

The material density γ_Ω is a piecewise constant function which takes two positive values:

$$\gamma_\Omega = \begin{cases} \gamma_{in} & \text{in } \Omega, \\ \gamma_{out} & \text{in } D \setminus \bar{\Omega}. \end{cases}$$

In the applications, $D \setminus \bar{\Omega}$ is occupied by a weak phase that approximates an empty region, thus we assume that

$$\gamma_{out} \ll \gamma_{in}. \quad (2.4)$$

The stress tensor $\sigma(u_\Omega)$, normalized to a unitary Young modulus, is related to the displacement field u_Ω through the Hooke law:

$$\sigma(u) = Ce(u),$$

where

$$e(u) = \frac{\nabla u + \nabla u^T}{2}$$

is the strain tensor, and

$$C = 2\mu \mathbb{I} + \lambda(I \otimes I)$$

is the elasticity tensor. Here, I and \mathbb{I} are the second and fourth order identity tensors, respectively, and the Lamé coefficients μ and λ are given in plane stress by

$$\mu = \frac{1}{2(1+\nu)}, \quad \text{and} \quad \lambda = \frac{\nu}{1-\nu^2},$$

where ν is the Poisson ratio. The Neumann data g is assumed to belong to $L^2(\Gamma_N)^2$. The Von Mises stress $\sigma_M(u)$ is given by

$$\sigma_M(u) = \sqrt{\frac{1}{2}\tilde{B}\sigma(u)\cdot\sigma(u)} = \sqrt{\frac{1}{2}B\sigma(u)\cdot e(u)},$$

where

$$\tilde{B} = 3\mathbb{I} - (I \otimes I) \quad (2.5)$$

and

$$B = C\tilde{B} = 6\mu\mathbb{I} + (\lambda - 2\mu)(I \otimes I). \quad (2.6)$$

The set \tilde{D} is an open subset of D and $\bar{\sigma}_M$ is a prescribed positive number. Finally, the objective functional $I_\Omega : \mathcal{V} \rightarrow \mathbb{R}$ is assumed to admit a known topological derivative $D_T I_\Omega$ as defined in Section 2.3.

2.2. Penalization of the constraint. Problem (2.1)-(2.3) is very difficult to address directly because of the pointwise constraint. Therefore we propose an approximation based on the introduction of a penalty functional. Let $\Phi : \mathbb{R}_+ \rightarrow \mathbb{R}_+$ be a nondecreasing function of class \mathcal{C}^2 . To enable proper justifications of the subsequent analysis, we assume further that the derivatives Φ' and Φ'' are bounded. We consider the penalty functional:

$$J_\Omega(u) = \int_{\tilde{D}} \gamma_\Omega \Phi\left(\frac{1}{2}B\sigma(u)\cdot e(u)\right) dx. \quad (2.7)$$

Then, given a penalty coefficient $\alpha > 0$, we define the penalized objective functional:

$$I_\Omega^\alpha(u) = I_\Omega(u) + \alpha J_\Omega(u).$$

Henceforth we shall solve the problem:

$$\text{Minimize } I_\Omega^\alpha(u_\Omega) \quad \text{subject to (2.2)}. \quad (2.8)$$

We will see that solving (2.8) instead of (2.1)-(2.3) leads to feasible domains provided that α and Φ are appropriately chosen, namely that the two following conditions are fulfilled:

- α is large enough,
- Φ' admits a sharp variation around $\bar{\sigma}$.

2.3. Topology perturbations. Given a point $x_0 \in D \setminus \partial\Omega$ and a radius $\varepsilon > 0$, we consider a circular inclusion $\omega_\varepsilon = B(x_0, \varepsilon)$, and we define the perturbed domain (see Fig. 1):

$$\Omega_\varepsilon = \begin{cases} \Omega \setminus \overline{\omega_\varepsilon} & \text{if } x_0 \in \Omega, \\ (\Omega \cup \omega_\varepsilon) \cap D & \text{if } x_0 \in D \setminus \overline{\Omega}. \end{cases}$$

We denote for simplicity $(u_{\Omega_\varepsilon}, \gamma_{\Omega_\varepsilon})$ by $(u_\varepsilon, \gamma_\varepsilon)$ and $(u_\Omega, \gamma_\Omega)$ by (u_0, γ_0) . Then, for all $\varepsilon \in [0, 1]$, γ_ε can be expressed as:

$$\gamma_\varepsilon = \begin{cases} \gamma_0 & \text{in } D \setminus \overline{\omega_\varepsilon}, \\ \gamma_1 & \text{in } \omega_\varepsilon. \end{cases}$$

We note that γ_0 and γ_1 are two positive functions defined in D and constant in a neighborhood of x_0 . For all $\varepsilon \geq 0$, the state equations can be rewritten:

$$\begin{cases} -\text{div}(\gamma_\varepsilon \sigma(u_\varepsilon)) = 0 & \text{in } D, \\ u_\varepsilon = 0 & \text{on } \Gamma_D, \\ \gamma_\varepsilon \sigma(u_\varepsilon) n = g & \text{on } \Gamma_N, \\ \sigma(u_\varepsilon) n = 0 & \text{on } \Gamma_0. \end{cases} \quad (2.9)$$

In order to solve (2.8), we are looking for an asymptotic expansion, named as topological asymptotic expansion, of the form

$$I_{\Omega_\varepsilon}^\alpha(u_\varepsilon) - I_\Omega^\alpha(u_0) = f(\varepsilon) D_T I_\Omega^\alpha(x_0) + o(f(\varepsilon)),$$

where $f : \mathbb{R}_+ \rightarrow \mathbb{R}_+$ is a function that goes to zero with ε , and $D_T I_\Omega^\alpha : D \rightarrow \mathbb{R}$ is the so-called topological derivative of the functional I_Ω^α . Since such an expansion is assumed to be known for

the objective functional I_Ω , we subsequently focus on the penalty functional J_Ω . We adopt the simplified notation:

$$J_\varepsilon(u) := J_{\Omega_\varepsilon}(u) = \int_{\tilde{D}} \gamma_\varepsilon \Phi\left(\frac{1}{2} B\sigma(u) \cdot e(u)\right) dx. \quad (2.10)$$

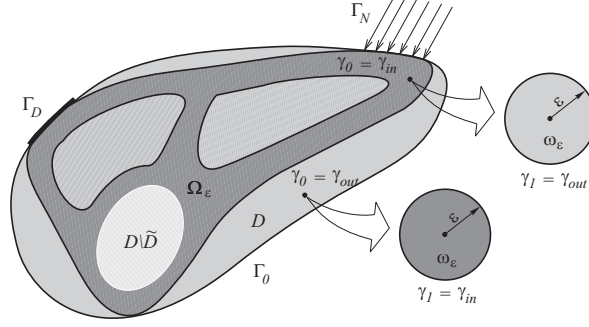


FIGURE 1. Sketch of the working domain.

3. TOPOLOGICAL SENSITIVITY ANALYSIS OF THE VON MISES STRESS PENALTY FUNCTIONAL

In this section, the topological sensitivity analysis of the penalty functional J_Ω is carried out. We follow the approach described in [8] for the Laplace problem. Here, the calculations are more technical, but the estimates of the remainders detached from the topological asymptotic expansion are analogous. Hence we do not repeat these estimates. The reader interested in the complete proofs may refer to [8].

Possibly shifting the origin of the coordinate system, we assume henceforth for simplicity that $x_0 = 0$.

3.1. A preliminary result. The reader interested in the proof of the proposition below may refer to [6].

Proposition 3.1. *Let \mathcal{V} be a Hilbert space and $\varepsilon_0 > 0$. For all $\varepsilon \in [0, \varepsilon_0)$, consider a vector $u_\varepsilon \in \mathcal{V}$ solution of a variational problem of the form*

$$a_\varepsilon(u_\varepsilon, v) = \ell_\varepsilon(v) \quad \forall v \in \mathcal{V}, \quad (3.1)$$

where a_ε and ℓ_ε are a bilinear form on \mathcal{V} and a linear form on \mathcal{V} , respectively. Consider also, for all $\varepsilon \in [0, \varepsilon_0)$, a functional $J_\varepsilon : \mathcal{V} \rightarrow \mathbb{R}$ and a linear form $L_\varepsilon(u_0) \in \mathcal{V}'$. Suppose that the following hypotheses hold.

- (1) *There exist two numbers δa and $\delta \ell$ and a function $\varepsilon \in \mathbb{R}_+ \mapsto f(\varepsilon) \in \mathbb{R}$ such that, when ε goes to zero,*

$$(a_\varepsilon - a_0)(u_0, v_\varepsilon) = f(\varepsilon)\delta a + o(f(\varepsilon)), \quad (3.2)$$

$$(\ell_\varepsilon - \ell_0)(v_\varepsilon) = f(\varepsilon)\delta \ell + o(f(\varepsilon)), \quad (3.3)$$

$$\lim_{\varepsilon \rightarrow 0} f(\varepsilon) = 0, \quad (3.4)$$

where $v_\varepsilon \in \mathcal{V}$ is an adjoint state satisfying

$$a_\varepsilon(\varphi, v_\varepsilon) = -\langle L_\varepsilon(u_0), \varphi \rangle \quad \forall \varphi \in \mathcal{V}. \quad (3.5)$$

- (2) *There exist two numbers δJ_1 and δJ_2 such that*

$$J_\varepsilon(u_\varepsilon) = J_\varepsilon(u_0) + \langle L_\varepsilon(u_0), u_\varepsilon - u_0 \rangle + f(\varepsilon)\delta J_1 + o(f(\varepsilon)), \quad (3.6)$$

$$J_\varepsilon(u_0) = J_0(u_0) + f(\varepsilon)\delta J_2 + o(f(\varepsilon)). \quad (3.7)$$

Then we have

$$J_\varepsilon(u_\varepsilon) - J_0(u_0) = f(\varepsilon)(\delta a - \delta \ell + \delta J_1 + \delta J_2) + o(f(\varepsilon)).$$

3.2. Adjoint state. The bilinear and linear forms associated with Problem (2.9) are classically defined in the space $\mathcal{V} = \{u \in H^1(D)^2, u|_{\Gamma_D} = 0\}$ by:

$$a_\varepsilon(u, v) = \int_D \gamma_\varepsilon \sigma(u) \cdot e(v) \, dx \quad \forall u, v \in \mathcal{V}, \quad (3.8)$$

$$\ell_\varepsilon(v) = \int_{\Gamma_N} g \cdot v \, ds \quad \forall v \in \mathcal{V}. \quad (3.9)$$

At the point u_0 (unperturbed solution), the penalty functional admits the tangent linear approximation $L_\varepsilon(u_0)$ given by:

$$\langle L_\varepsilon(u_0), \varphi \rangle = \int_{\tilde{D}} \gamma_\varepsilon \Phi' \left(\frac{1}{2} B \sigma(u_0) \cdot e(u_0) \right) B \sigma(u_0) \cdot e(\varphi) \, dx \quad \forall \varphi \in \mathcal{V}.$$

We define the function

$$k_1 = \Phi' \left(\frac{1}{2} B \sigma(u_0) \cdot e(u_0) \right) \chi_{\tilde{D}}, \quad (3.10)$$

where $\chi_{\tilde{D}}$ is the characteristic function of \tilde{D} . Then the adjoint state is (a weak) solution of the boundary value problem:

$$\begin{cases} -\operatorname{div} (\gamma_\varepsilon \sigma(v_\varepsilon)) = +\operatorname{div} (\gamma_\varepsilon k_1 B \sigma(u_0)) & \text{in } D, \\ v_\varepsilon = 0 & \text{on } \Gamma_D, \\ \gamma_\varepsilon \sigma(v_\varepsilon) n = -\gamma_\varepsilon k_1 B \sigma(u_0) n & \text{on } \Gamma_N \cup \Gamma_0. \end{cases} \quad (3.11)$$

3.3. Regularity assumptions. We make the following assumptions.

- (1) For any $r_1 > 0$ there exists $r_2 \in (0, r_1)$ such that every function $u \in H^1(D \setminus \overline{B(x_0, r_2)})^2$ satisfying

$$\begin{cases} -\operatorname{div} (\gamma_0 \sigma(u)) = 0 & \text{in } D \setminus \overline{B(x_0, r_2)}, \\ u = 0 & \text{on } \Gamma_D, \\ \gamma_0 \sigma(u_\varepsilon) n = 0 & \text{on } \Gamma_N \cup \Gamma_0 \end{cases}$$

belongs to $W^{1,4}(\tilde{D} \setminus \overline{B(x_0, r_1)})^2$.

- (2) The load g is such that $u_0 \in W^{1,4}(\tilde{D})^2$.

Note that, by elliptic regularity, u_0 and v_0 are automatically of class $\mathcal{C}^{1,\beta}$, $\beta > 0$, in the vicinity of x_0 provided that $x_0 \in D \setminus \partial\Omega \setminus \partial\tilde{D}$.

Remark 3.2. The above assumption is satisfied in many situations, including nonsmooth domains, like for instance in the following case:

- D is a Lipschitz polygon,
- $\Gamma_N \cap \partial\tilde{D} = \emptyset$ and $\Gamma_D \cap \partial\tilde{D} = \emptyset$,
- the interface $\partial\Omega \setminus \partial D$ is the disjoint union of smooth simple arcs,
- if a junction point between the interface and ∂D belongs to $\partial\tilde{D}$, then the Young modulus distribution around this point is quasi-monotone (see the definition in [27]); in particular, if only one arc touches ∂D at this point, it is sufficient that the angle defined by these curves in $D \setminus \overline{\Omega}$ is less than π .

We refer to [27] and the references therein for justifications and extensions.

3.4. Variation of the bilinear form. In order to apply Proposition 3.1, we need to obtain a closed form for the leading term of the quantity:

$$(a_\varepsilon - a_0)(u_0, v_\varepsilon) = \int_{\omega_\varepsilon} (\gamma_1 - \gamma_0) \sigma(u_0) \cdot e(v_\varepsilon) \, dx. \quad (3.12)$$

In the course of the analysis, the remainders detached from this expression will be denoted by $\mathcal{E}_i(\varepsilon)$, $i = 1, 2, \dots$. By setting $\tilde{v}_\varepsilon = v_\varepsilon - v_0$ and assuming that ε is sufficiently small so that γ_ε is constant in ω_ε , we obtain:

$$(a_\varepsilon - a_0)(u_0, v_\varepsilon) = (\gamma_1 - \gamma_0)(x_0) \left(\int_{\omega_\varepsilon} \sigma(u_0) \cdot e(v_0) \, dx + \int_{\omega_\varepsilon} \sigma(u_0) \cdot e(\tilde{v}_\varepsilon) \, dx \right).$$

For the reader's convenience, the values of $\gamma_0(x_0)$ and $\gamma_1(x_0)$ are reported in Table 1 (see also Fig. 1). Since u_0 and v_0 are smooth in the vicinity of x_0 , we approximate $\sigma(u_0)$ and $e(v_0)$ in

x_0	$\gamma_0(x_0)$	$\gamma_1(x_0)$
Ω	γ_{in}	γ_{out}
$D \setminus \overline{\Omega}$	γ_{out}	γ_{in}

TABLE 1. Coefficients $\gamma_0(x_0)$ and $\gamma_1(x_0)$ according to the location of x_0 .

the first integral by their values at the point x_0 , and write:

$$(a_\varepsilon - a_0)(u_0, v_\varepsilon) = (\gamma_1 - \gamma_0)(x_0) \left(\pi \varepsilon^2 \sigma(u_0)(x_0) \cdot e(v_0)(x_0) + \int_{\omega_\varepsilon} \sigma(u_0) \cdot e(\tilde{v}_\varepsilon) dx + \mathcal{E}_1(\varepsilon) \right).$$

As v_ε is solution of the adjoint equation (3.11), then the function \tilde{v}_ε solves

$$\begin{cases} -\operatorname{div}(\gamma_\varepsilon \sigma(\tilde{v}_\varepsilon)) = 0 & \text{in } \omega_\varepsilon \cup (D \setminus \overline{\omega_\varepsilon}), \\ [\gamma_\varepsilon \sigma(\tilde{v}_\varepsilon)n] = -(\gamma_1 - \gamma_0)(k_1 B \sigma(u_0)n + \sigma(v_0)n) & \text{on } \partial\omega_\varepsilon, \\ \tilde{v}_\varepsilon = 0 & \text{on } \Gamma_D, \\ \sigma(\tilde{v}_\varepsilon)n = 0 & \text{on } \Gamma_N \cup \Gamma_0, \end{cases} \quad (3.13)$$

where $[\gamma_\varepsilon \sigma(\tilde{v}_\varepsilon)n] \in H^{-1/2}(\partial\omega_\varepsilon)^2$ denotes the jump of the normal stress through the interface $\partial\omega_\varepsilon$. We recall that, as before, the boundary value problem (3.13) is to be understood in the weak sense for $\tilde{v}_\varepsilon \in H^1(D)^2$. We set $S = S_1 + S_2$, with

$$S_1 = k_1(x_0)B\sigma(u_0)(x_0) \quad \text{and} \quad S_2 = \sigma(v_0)(x_0).$$

We approximate $\sigma(\tilde{v}_\varepsilon)$ by $\sigma(h_\varepsilon^S)$ solution of the auxiliary problem:

$$\begin{cases} -\operatorname{div} \sigma(h_\varepsilon^S) = 0 & \text{in } \omega_\varepsilon \cup (\mathbb{R}^2 \setminus \overline{\omega_\varepsilon}), \\ [\gamma_\varepsilon \sigma(h_\varepsilon^S)n] = -(\gamma_1 - \gamma_0)(x_0)Sn & \text{on } \partial\omega_\varepsilon, \\ \sigma(h_\varepsilon^S) \rightarrow 0 & \text{at } \infty. \end{cases} \quad (3.14)$$

In the present case of a circular inclusion, the tensor $\sigma(h_\varepsilon^S)$ admits the following expression in a polar coordinate system (r, θ) :

- for $r \geq \varepsilon$

$$\sigma_r(r, \theta) = -(\alpha_1 + \alpha_2) \frac{1 - \gamma}{1 + \xi\gamma} \frac{\varepsilon^2}{r^2} - \frac{1 - \gamma}{1 + \eta\gamma} \left(4 \frac{\varepsilon^2}{r^2} - 3 \frac{\varepsilon^4}{r^4} \right) (\beta_1 \cos 2\theta + \beta_2 \cos 2(\theta + \delta)) \quad (3.15)$$

$$\sigma_\theta(r, \theta) = (\alpha_1 + \alpha_2) \frac{1 - \gamma}{1 + \xi\gamma} \frac{\varepsilon^2}{r^2} - 3 \frac{1 - \gamma}{1 + \eta\gamma} \frac{\varepsilon^4}{r^4} (\beta_1 \cos 2\theta + \beta_2 \cos 2(\theta + \delta)), \quad (3.16)$$

$$\sigma_{r\theta}(r, \theta) = -\frac{1 - \gamma}{1 + \eta\gamma} \left(2 \frac{\varepsilon^2}{r^2} - 3 \frac{\varepsilon^4}{r^4} \right) (\beta_1 \sin 2\theta + \beta_2 \sin 2(\theta + \delta)), \quad (3.17)$$

- for $0 < r < \varepsilon$

$$\sigma_r(r, \theta) = (\alpha_1 + \alpha_2) \xi \frac{1 - \gamma}{1 + \xi\gamma} + \eta \frac{1 - \gamma}{1 + \eta\gamma} (\beta_1 \cos 2\theta + \beta_2 \cos 2(\theta + \delta)), \quad (3.18)$$

$$\sigma_\theta(r, \theta) = (\alpha_1 + \alpha_2) \xi \frac{1 - \gamma}{1 + \xi\gamma} - \eta \frac{1 - \gamma}{1 + \eta\gamma} (\beta_1 \cos 2\theta + \beta_2 \cos 2(\theta + \delta)), \quad (3.19)$$

$$\sigma_{r\theta}(r, \theta) = -\eta \frac{1 - \gamma}{1 + \eta\gamma} (\beta_1 \sin 2\theta + \beta_2 \sin 2(\theta + \delta)), \quad (3.20)$$

Some terms in the above formulas require explanation. The parameter δ denotes the angle between the eigenvectors of tensors S_1 and S_2 ,

$$\alpha_i = \frac{1}{2}(s_I^i + s_{II}^i) \quad \text{and} \quad \beta_i = \frac{1}{2}(s_I^i - s_{II}^i), \quad i = 1, 2,$$

where s_I^i and s_{II}^i are the eigenvalues of tensors S_i for $i = 1, 2$. In addition, the constants ξ and η are respectively given by

$$\xi = \frac{1 + \nu}{1 - \nu}, \quad \eta = \frac{3 - \nu}{1 + \nu},$$

and γ is the contrast, that is, $\gamma = \gamma_1(x_0)/\gamma_0(x_0)$.

From these elements, we obtain successively:

$$\int_{\omega_\varepsilon} \sigma(u_0).e(\tilde{v}_\varepsilon)dx = \int_{\omega_\varepsilon} \sigma(\tilde{v}_\varepsilon).e(u_0)dx = \int_{\omega_\varepsilon} \sigma(h_\varepsilon^S).e(u_0)dx + \mathcal{E}_2(\varepsilon).$$

Then approximating $e(u_0)$ in ω_ε by its value at x_0 and calculating the resulting integral with the help of the expressions (3.18)-(3.20) yields:

$$\begin{aligned} \int_{\omega_\varepsilon} \sigma(u_0).e(\tilde{v}_\varepsilon)dx &= \int_{\omega_\varepsilon} \sigma(h_\varepsilon^S).e(u_0)(x_0)dx + \mathcal{E}_2(\varepsilon) + \mathcal{E}_3(\varepsilon) \\ &= -\pi\varepsilon^2\rho(k_1TB\sigma(u_0).e(u_0) + T\sigma(u_0).e(v_0))(x_0) + \mathcal{E}_2(\varepsilon) + \mathcal{E}_3(\varepsilon), \end{aligned}$$

with

$$\rho = \frac{\gamma_1 - \gamma_0}{\eta\gamma_1 + \gamma_0}(x_0) \quad \text{and} \quad T = \eta I + \frac{1}{2} \frac{\xi - \eta}{1 + \gamma\xi} I \otimes I. \quad (3.21)$$

Finally, the variation of the bilinear form can be written in the form:

$$\begin{aligned} (a_\varepsilon - a_0)(u_0, v_\varepsilon) &= -\pi\varepsilon^2(\gamma_1 - \gamma_0)(x_0)\rho \left(k_1\eta B\sigma(u_0).e(u_0) + \frac{1}{2}k_1 \frac{\xi - \eta}{1 + \gamma\xi} \text{tr}B\sigma(u_0)\text{tr}e(u_0) \right. \\ &\quad \left. - \frac{\eta + 1}{\gamma - 1}\sigma(u_0).e(v_0) + \frac{1}{2} \frac{\xi - \eta}{1 + \gamma\xi} \text{tr}\sigma(u_0)\text{tr}e(v_0) \right) (x_0) + (\gamma_1 - \gamma_0)(x_0) \sum_{i=1}^3 \mathcal{E}_i(\varepsilon). \end{aligned} \quad (3.22)$$

3.5. Variation of the linear form. Since here ℓ_ε is independent of ε , it follows trivially that

$$(\ell_\varepsilon - \ell_0)(v_\varepsilon) = 0. \quad (3.23)$$

3.6. Partial variation of the penalty functional with respect to the state. We now study the variation:

$$\begin{aligned} V_{J1}(\varepsilon) &:= J_\varepsilon(u_\varepsilon) - J_\varepsilon(u_0) - \langle L_\varepsilon(u_0), u_\varepsilon - u_0 \rangle \\ &= \int_{\tilde{D}} \gamma_\varepsilon \left[\Phi\left(\frac{1}{2}B\sigma(u_\varepsilon).e(u_\varepsilon)\right) - \Phi\left(\frac{1}{2}B\sigma(u_0).e(u_0)\right) - \Phi'\left(\frac{1}{2}B\sigma(u_0).e(u_0)\right)B\sigma(u_0).e(u_\varepsilon - u_0) \right] dx. \end{aligned}$$

By setting $\tilde{u}_\varepsilon = u_\varepsilon - u_0$, we can write:

$$\begin{aligned} V_{J1}(\varepsilon) &= \int_{\tilde{D}} \gamma_\varepsilon \left[\Phi\left(\frac{1}{2}B\sigma(u_0).e(u_0) + B\sigma(u_0).e(\tilde{u}_\varepsilon) + \frac{1}{2}B\sigma(\tilde{u}_\varepsilon).e(\tilde{u}_\varepsilon)\right) - \Phi\left(\frac{1}{2}B\sigma(u_0).e(u_0)\right) \right. \\ &\quad \left. - \Phi'\left(\frac{1}{2}B\sigma(u_0).e(u_0)\right)B\sigma(u_0).e(\tilde{u}_\varepsilon) \right] dx. \end{aligned} \quad (3.24)$$

Since u_ε is solution of the state equation (2.9), then by difference we find that \tilde{u}_ε solves:

$$\begin{cases} -\text{div}(\gamma_\varepsilon\sigma(\tilde{u}_\varepsilon)) &= 0 & \text{in } \omega_\varepsilon \cup (D \setminus \overline{\omega_\varepsilon}), \\ [\gamma_\varepsilon\sigma(\tilde{u}_\varepsilon)n] &= -(\gamma_1 - \gamma_0)\sigma(u_0)n & \text{on } \partial\omega_\varepsilon, \\ \tilde{u}_\varepsilon &= 0 & \text{on } \Gamma_D, \\ \sigma(\tilde{u}_\varepsilon)n &= 0 & \text{on } \Gamma_N \cup \Gamma_0. \end{cases} \quad (3.25)$$

By setting now $S = \sigma(u_0)(x_0)$, we approximate \tilde{u}_ε by h_ε^S solution of the auxiliary problem (3.14). It comes:

$$\begin{aligned} V_{J1}(\varepsilon) &= \int_{\tilde{D}} \gamma_\varepsilon \left[\Phi\left(\frac{1}{2}B\sigma(u_0).e(u_0) + B\sigma(u_0).e(h_\varepsilon^S) + \frac{1}{2}B\sigma(h_\varepsilon^S).e(h_\varepsilon^S)\right) - \Phi\left(\frac{1}{2}B\sigma(u_0).e(u_0)\right) \right. \\ &\quad \left. - \Phi'\left(\frac{1}{2}B\sigma(u_0).e(u_0)\right)B\sigma(u_0).e(h_\varepsilon^S) \right] dx + \mathcal{E}_4(\varepsilon). \end{aligned} \quad (3.26)$$

If $x_0 \in D \setminus \overline{\tilde{D}}$, we obtain easily, using a Taylor expansion of Φ and the estimate $|\sigma(h_\varepsilon^S)(x)| = O(\varepsilon^2)$ which holds uniformly with respect to x a fixed distance away from x_0 , that $V_{J1}(\varepsilon) = o(\varepsilon^2)$. Thus we assume that $x_0 \in \tilde{D}$ (the special case where $x_0 \in \partial\tilde{D}$ is not treated). In view of the decay of $\sigma(h_\varepsilon^S)$ at infinity and the regularity of u_0 near x_0 , we write

$$V_{J1}(\varepsilon) = \int_{\mathbb{R}^2} \gamma_\varepsilon^* \left[\Phi\left(\frac{1}{2}B\sigma(u_0)(x_0).e(u_0)(x_0) + B\sigma(u_0)(x_0).e(h_\varepsilon^S) + \frac{1}{2}B\sigma(h_\varepsilon^S).e(h_\varepsilon^S)\right) - \Phi\left(\frac{1}{2}B\sigma(u_0)(x_0).e(u_0)(x_0)\right) - \Phi'\left(\frac{1}{2}B\sigma(u_0)(x_0).e(u_0)(x_0)\right)B\sigma(u_0)(x_0).e(h_\varepsilon^S) \right] dx + \mathcal{E}_4(\varepsilon) + \mathcal{E}_5(\varepsilon),$$

with $\gamma_\varepsilon^*(x) = \gamma_1(x_0)$ if $x \in \omega_\varepsilon$, $\gamma_\varepsilon^*(x) = \gamma_0(x_0)$ otherwise. The above expression can be rewritten as

$$V_{J1}(\varepsilon) = \int_{\mathbb{R}^2} \gamma_\varepsilon^* \left[\Phi\left(\frac{1}{2}\tilde{B}S.S + \tilde{B}S.\sigma(h_\varepsilon^S) + \frac{1}{2}\tilde{B}\sigma(h_\varepsilon^S).\sigma(h_\varepsilon^S)\right) - \Phi\left(\frac{1}{2}\tilde{B}S.S\right) - \Phi'\left(\frac{1}{2}\tilde{B}S.S\right)\tilde{B}S.\sigma(h_\varepsilon^S) \right] dx + \mathcal{E}_4(\varepsilon) + \mathcal{E}_5(\varepsilon).$$

We denote by $V_{J11}(\varepsilon)$ and $V_{J12}(\varepsilon)$ the parts of the above integral computed over ω_ε and $\mathbb{R}^2 \setminus \overline{\omega_\varepsilon}$, respectively. Using the expressions (3.18)-(3.20), we find

$$V_{J11}(\varepsilon) = \pi\varepsilon^2\gamma_1(x_0) \left[\Phi\left(\frac{1}{2}\tilde{B}S.S - \rho T\tilde{B}S.S + \rho^2\frac{1}{2}T\tilde{B}TS.S\right) - \Phi\left(\frac{1}{2}\tilde{B}S.S\right) + \rho\Phi'\left(\frac{1}{2}\tilde{B}S.S\right)T\tilde{B}S.S \right].$$

Next, we define the function independent of ε

$$\Sigma_\rho^S(x) = \sigma(h_\varepsilon^S)(\varepsilon x). \quad (3.27)$$

A change of variable yields

$$V_{J12}(\varepsilon) = \varepsilon^2 \int_{\mathbb{R}^2 \setminus \overline{\omega}} \gamma_0(x_0) \left[\Phi\left(\frac{1}{2}\tilde{B}S.S + \tilde{B}S.\Sigma_\rho^S + \frac{1}{2}\tilde{B}\Sigma_\rho^S.\Sigma_\rho^S\right) - \Phi\left(\frac{1}{2}\tilde{B}S.S\right) - \Phi'\left(\frac{1}{2}\tilde{B}S.S\right)\tilde{B}S.\Sigma_\rho^S \right] dx.$$

We set

$$\Psi_\rho(S) = \int_{\mathbb{R}^2 \setminus \overline{\omega}} \left[\Phi\left(\frac{1}{2}\tilde{B}S.S + \tilde{B}S.\Sigma_\rho^S + \frac{1}{2}\tilde{B}\Sigma_\rho^S.\Sigma_\rho^S\right) - \Phi\left(\frac{1}{2}\tilde{B}S.S\right) - \Phi'\left(\frac{1}{2}\tilde{B}S.S\right)(\tilde{B}S.\Sigma_\rho^S + \frac{1}{2}\tilde{B}\Sigma_\rho^S.\Sigma_\rho^S) \right] dx. \quad (3.28)$$

The extra term $\frac{1}{2}\tilde{B}\Sigma_\rho^S.\Sigma_\rho^S$ has been added so that $\Psi_\rho(S)$ vanishes whenever Φ is linear. Thus we have

$$V_{J12}(\varepsilon) = \varepsilon^2\gamma_0(x_0) \left[\Psi_\rho(S) + \frac{1}{2}\Phi'\left(\frac{1}{2}\tilde{B}S.S\right) \int_{\mathbb{R}^2 \setminus \overline{\omega}} \tilde{B}\Sigma_\rho^S.\Sigma_\rho^S dx \right].$$

Using the expressions (3.15)-(3.17), a symbolic calculation of the above integral provides

$$V_{J12}(\varepsilon) = \varepsilon^2\gamma_0(x_0) \left[\Psi_\rho(S) + \frac{1}{4}\pi\rho^2k_1(x_0) \left(5(2S.S - \text{tr}^2S) + 3\left(\frac{1+\eta\gamma}{1+\xi\gamma}\right)^2 \text{tr}^2S \right) \right].$$

Besides, after a change of variable and rearrangements, $\Psi_\rho(S)$ reduces to

$$\Psi_\rho(S) = \int_0^1 \int_0^\pi \frac{1}{t^2} [\Phi(s_M^2 + \Delta(t, \theta)) - \Phi(s_M^2) - \Phi'(s_M^2)\Delta(t, \theta)] d\theta dt, \quad (3.29)$$

where

$$\begin{aligned} \Delta(t, \theta) &= \rho\frac{t}{2} \left[(s_I^2 - s_{II}^2)(2 + 3\frac{1+\eta\gamma}{1+\xi\gamma}) \cos\theta + 3(s_I - s_{II})^2(2 - 3t) \cos 2\theta \right] \\ &+ \rho^2\frac{t^2}{4} \left[3(s_I + s_{II})^2\left(\frac{1+\eta\gamma}{1+\xi\gamma}\right)^2 + (s_I - s_{II})^2(3(2 - 3t)^2 + 4\cos^2\theta) + 6\frac{1+\eta\gamma}{1+\xi\gamma}(s_I^2 - s_{II}^2)(2 - 3t) \cos\theta \right], \\ s_M^2 &= \frac{1}{2}\tilde{B}S.S. \end{aligned}$$

Finally we obtain:

$$\begin{aligned}
VJ_1(\varepsilon) &= \pi\gamma_1(x_0) \left[\Phi\left(\frac{1}{2}\tilde{B}S.S - \rho T\tilde{B}S.S + \rho^2\frac{1}{2}T\tilde{B}TS.S\right) - \Phi\left(\frac{1}{2}\tilde{B}S.S\right) + \rho\Phi'\left(\frac{1}{2}\tilde{B}S.S\right)T\tilde{B}S.S \right] \\
&+ \gamma_0(x_0) \left[\Psi_\rho(S) + \frac{1}{4}\pi\rho^2k_1(x_0) \left(5(2S.S - \text{tr}^2S) + 3\left(\frac{1+\eta\gamma}{1+\xi\gamma}\right)^2 \text{tr}^2S \right) \right] + \mathcal{E}_4(\varepsilon) + \mathcal{E}_5(\varepsilon).
\end{aligned} \tag{3.30}$$

3.7. Partial variation of the penalty functional with respect to the domain. The last term is treated as follows:

$$\begin{aligned}
VJ_2(\varepsilon) &:= J_\varepsilon(u_0) - J_0(u_0) \\
&= \int_{\omega_\varepsilon \cap \tilde{D}} (\gamma_1 - \gamma_0) \Phi\left(\frac{1}{2}B\sigma(u_0).e(u_0)\right) dx \\
&= \pi\varepsilon^2\chi_{\tilde{D}}(x_0)(\gamma_1 - \gamma_0)(x_0)\Phi\left(\frac{1}{2}B\sigma(u_0)(x_0).e(u_0)(x_0)\right) + \mathcal{E}_6(\varepsilon).
\end{aligned}$$

3.8. Topological derivative. Like in [8] for the Laplace equation, we can prove that the reminders $\mathcal{E}_i(\varepsilon)$, $i = 1, \dots, 6$ behave like $o(\varepsilon^2)$. Therefore, after summation of the different terms according to Proposition 3.1 and a few simplifications, we arrive at the final formula for the topological asymptotic expansion of the penalty functional. It is given by

$$J_\varepsilon(u_\varepsilon) - J_0(u_0) = \varepsilon^2 D_T J_\Omega(x_0) + o(\varepsilon^2)$$

with the topological derivative

$$\begin{aligned}
D_T J_\Omega &= -\pi(\gamma_1 - \gamma_0) [\rho k_1 T B S.E + (\rho T - \mathbb{I}) S.E_a] \\
&+ \pi\gamma_1\chi_{\tilde{D}} \left[\Phi\left(\frac{1}{2}\tilde{B}S.S - \rho T\tilde{B}S.S + \rho^2\frac{1}{2}T\tilde{B}TS.S\right) + \rho k_1 T \tilde{B} S.S \right] \\
&+ \gamma_0\chi_{\tilde{D}} \left[\Psi_\rho(S) + \frac{1}{4}\pi\rho^2k_1 \left(5(2S.S - \text{tr}^2S) + 3\left(\frac{1+\eta\gamma}{1+\xi\gamma}\right)^2 \text{tr}^2S \right) \right] - \pi\chi_{\tilde{D}}\gamma_0\Phi\left(\frac{1}{2}\tilde{B}S.S\right).
\end{aligned} \tag{3.31}$$

Formula (3.31) is valid for all $x_0 \in D \setminus \partial\tilde{D} \setminus \partial\Omega$. We recall that ρ and T are given by (3.21); \tilde{B} , B , k_1 and $\Psi_\rho(S)$ are respectively given by (2.5), (2.6), (3.10), (3.29) and

$$S = \sigma(u_0), \quad E = e(u_0), \quad E_a = e(v_0).$$

The coefficients γ_0 and γ_1 are given by Table 1. Moreover, $u_0 = u_\Omega$ is the solution of the state equation (2.2) and $v_0 = v_\Omega$ is the solution of the adjoint equation (3.11) for $\varepsilon = 0$, that is,

$$\begin{cases} -\text{div}(\gamma_0\sigma(v_0)) = +\text{div}(\gamma_0k_1B\sigma(u_0)) & \text{in } D, \\ v_0 = 0 & \text{on } \Gamma_D, \\ \gamma_0\sigma(v_0)n = -\gamma_0k_1B\sigma(u_0)n & \text{on } \Gamma_N \cup \Gamma_0. \end{cases} \tag{3.32}$$

Remark 3.3. For the particular case in which $\nu = 1/3$, Formula (3.31) admits the simpler expression:

$$\begin{aligned}
D_T J_\Omega &= -\pi(\gamma_1 - \gamma_0) [4\rho k_1 s_M^2 - (1 - 2\rho) S.E_a] + \pi\gamma_1\chi_{\tilde{D}} \left[\Phi((1 - 2\rho)^2 s_M^2) + 4\rho k_1 s_M^2 \right] \\
&+ \gamma_0\chi_{\tilde{D}} \left[\Psi_\rho(S) + \frac{1}{2}\pi\rho^2k_1(5S.S - \text{tr}^2S) \right] - \pi\gamma_0\chi_{\tilde{D}}\Phi(s_M^2),
\end{aligned}$$

where $\Psi_\rho(S)$ is given by (3.29) with

$$\begin{aligned}
\Delta(t, \theta) &= \rho\frac{t}{2} [5(s_I^2 - s_{II}^2) \cos \theta + 3(s_I - s_{II})^2(2 - 3t) \cos 2\theta] \\
&+ \rho^2\frac{t^2}{4} [3(s_I + s_{II})^2 + (s_I - s_{II})^2(3(2 - 3t)^2 + 4 \cos^2 \theta) + 6(s_I^2 - s_{II}^2)(2 - 3t) \cos \theta]
\end{aligned}$$

and

$$\rho = \frac{\gamma_1 - \gamma_0}{2\gamma_1 + \gamma_0}(x_0).$$

Remark 3.4. Formula (3.31) has some similarity with results proved in [30], where a theory is developed for a broad class of elliptic state equations and shape functionals in three space dimensions, then it is applied to the linear elasticity case. However, the shape functionals addressed in this context are linear or quadratic in $\sigma(u)$, and there is no background material (the inclusions are Neumann holes).

4. A TOPOLOGY DESIGN ALGORITHM

Given a real parameter $p \geq 1$, we consider the penalty function (see Fig. 2):

$$\Phi_p(t) = \Theta_p\left(\frac{t}{\bar{\sigma}_M}\right)$$

with

$$\begin{aligned} \Theta_p : \mathbb{R}_+ &\rightarrow \mathbb{R}_+, \\ t &\mapsto (1 + t^p)^{1/p} - 1. \end{aligned}$$

It is clear that this function satisfies the required assumptions (see Section 2.2). The penalized

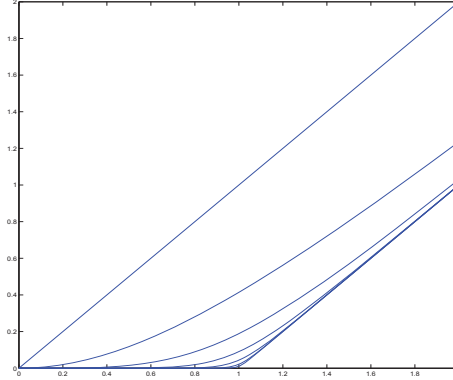


FIGURE 2. Function Θ_{p_n} for $p_n = 2^n$, $n = 0, \dots, 6$.

problem that we shall solve reads:

$$\text{Minimize}_{\Omega \subset D} I_\Omega^\alpha(u_\Omega) = I_\Omega(u_\Omega) + \alpha \int_{\bar{D}} \gamma_\Omega \Phi_p(\sigma_M(u_\Omega)^2) dx \quad \text{subject to (2.2)}. \quad (4.1)$$

In practice, p must be chosen as large as possible, provided that the resolution of (4.1) can accommodate with the sharp variation of Θ_p' around 1. In all the numerical examples, we take the value $p = 32$ which, after several trials, proved to be a good compromise. In order to reduce the computer time, the function Ψ_p has been tabulated (see Fig. 3).

The unconstrained minimization problem (4.1) is solved by using the algorithm devised in [7]. We briefly describe this algorithm here. It relies on a level-set domain representation and the approximation of topological optimality conditions by a fixed point method. Thus, the current domain Ω is characterized by a function $\psi \in L^2(D)$ such that $\Omega = \{x \in D, \psi(x) < 0\}$ and $D \setminus \bar{\Omega} = \{x \in D, \psi(x) > 0\}$. We compute the topological derivative $D_T I^\alpha(\Omega) = D_T I(\Omega) + \alpha D_T J(\Omega)$ where $D_T J(\Omega)$ is given by formula (3.31) with γ_0 and γ_1 chosen according to Table 1. Then we set $G(x) = D_T I^\alpha(\Omega)(x)$ if $x \in D \setminus \bar{\Omega}$ and $G(x) = -D_T I^\alpha(\Omega)(x)$ if $x \in \Omega$. We define the equivalence relation on $L^2(D)$:

$$\varphi \sim \psi \iff \exists \lambda > 0, \varphi = \lambda \psi.$$

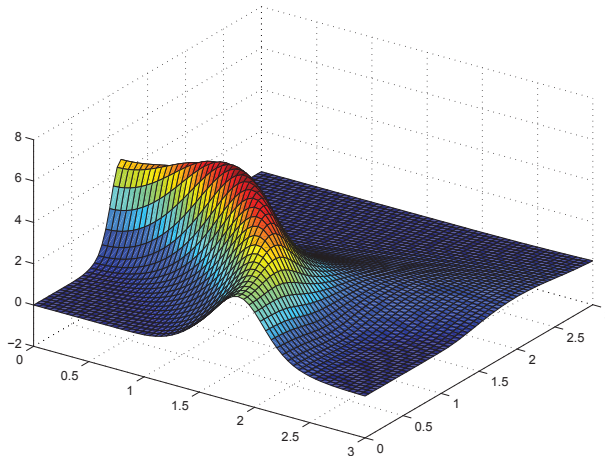


FIGURE 3. Function Ψ_ρ for $\rho = -1$ (hole creation), $p = 8$ and $\nu = 0.3$, with $s_I + s_{II}$ in abscissa and $s_I - s_{II}$ in ordinate.

Clearly, the relation $G \sim \psi$ is a sufficient optimality condition for the class of perturbations under consideration. We construct successive approximations of this condition by means of a sequence $(\psi_n)_{n \in \mathbb{N}}$ verifying

$$\begin{aligned} \psi_0 &\in L^2(D), \\ \psi_{n+1} &\in \text{co}(\psi_n, G_n) \quad \forall n \in \mathbb{N}. \end{aligned}$$

Above, the convex hull $\text{co}(\psi_n, G_n)$ applies to the equivalence classes, namely half-lines. Choosing representatives of unitary norm for ψ_n , ψ_{n+1} and G_n , we obtain the algorithm:

$$\begin{aligned} \psi_0 &\in \mathcal{S}, \\ \psi_{n+1} &= \frac{1}{\sin \theta_n} [\sin((1 - \kappa_n)\theta_n)\psi_n + \sin(\kappa_n\theta_n)G_n] \quad \forall n \in \mathbb{N}. \end{aligned}$$

The notations are the following: \mathcal{S} is the unit sphere of $L^2(D)$, $\theta_n = \arccos \frac{\langle G_n, \psi_n \rangle}{\|G_n\| \|\psi_n\|}$ is the angle between the vectors G_n and ψ_n , and $\kappa_n \in [0, 1]$ is a step which is determined by a line search in order to decrease the penalized objective functional. The iterations are stopped when this decrease becomes too small. At this stage, if the optimality condition is not approximated in a satisfactory manner (namely the angle θ_n is too large), an adaptive mesh refinement using a residual based a posteriori error estimate on the solution u_{Ω_n} is performed and the algorithm is continued.

5. NUMERICAL EXPERIMENTS

Given a fixed multiplier $\beta > 0$, we consider the objective functional

$$I_\Omega(u_\Omega) = |\Omega| + \beta K(u_\Omega),$$

with $|\Omega|$ the area of Ω and the compliance

$$K(u_\Omega) = \int_{\Gamma_N} g \cdot u_\Omega ds.$$

Unless otherwise specified, the domain \tilde{D} is equal to the whole computational domain D . The material densities are $\gamma_{in} = 1$ and $\gamma_{out} = 10^{-3}$. The Poisson ratio is $\nu = 0.3$. The topological derivative of the area is obvious, and that of the compliance is known (see [6, 21]). In each case, the initial guess is the full domain $\Omega_0 = D$.

5.1. **Bar.** Our first example is a bar under traction (see Fig. 4). The computational domain is the unit square and the load is uniformly distributed along two line segments of length 0.4. For comparison, we first address the unconstrained situation (*i.e.* $\alpha = 0$). We choose $\beta = 1$, so that the theoretical optimal domain is known as the horizontal central band of width 0.4. Next, we want to retrieve this domain with the local stress constraint $\sigma_M(u_\Omega) \leq \bar{\sigma}_M = 1$, and β comprised between 0 and 1. We choose $\beta = 0.2$ and $\alpha = 1$, then $\alpha = 10$. We observe that the obtained domains satisfy the constraint, but they are slightly bigger than the theoretical optimum. This is a consequence of the fact that $\Theta_p(s)$ is slightly positive for $s < 1$. For those three computations, the CPU time used on a PC with 2.4 GHz processor is equal to 90s, 110s and 114s, respectively, for a mesh containing 12961 nodes.

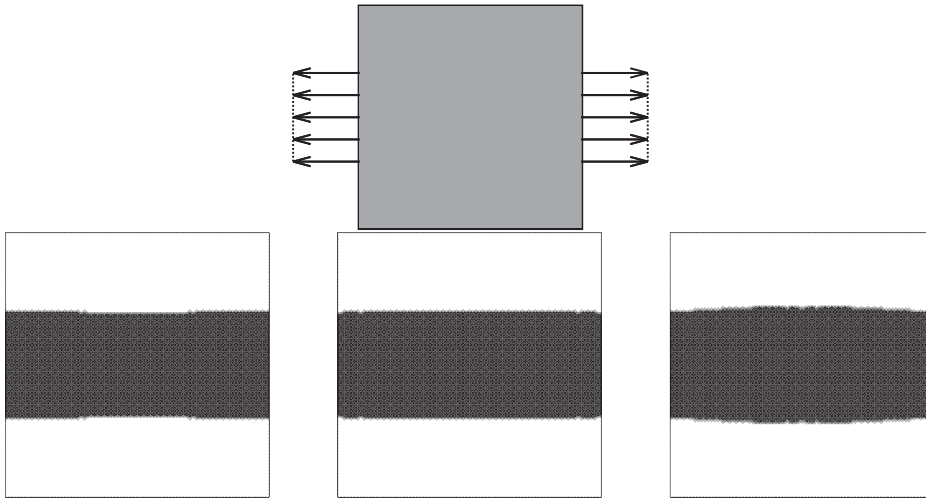


FIGURE 4. Bar: boundary conditions and obtained domains for $(\alpha, \beta) = (0, 1)$, $(\alpha, \beta) = (1, 0.2)$ and $(\alpha, \beta) = (10, 0.2)$, respectively.

5.2. **Michell's structure.** We study a variant of Michell's structure constructed in order to avoid any stress singularity at the initial stage. The working domain is a rectangle of size 65×80 perforated by two circular holes (see Fig. 5, left). On the left one a Dirichlet boundary condition is prescribed. On the right one a surface load of density $g = (0, -1)^T$ is applied. We address the unconstrained and constrained cases successively (see Fig. 5 and Fig. 6). In the second case, we take $\bar{\sigma}_M = 6$, $\beta = 0.04$ and $\alpha = 100$ then $\alpha = 500$. In the first case, we take $\beta = 0.078$ so as to obtain a structure with similar area to the previous case ($\alpha = 100$). Some numerical data are reported in Table 2 for comparison. The last column indicates the number of nodes in the final mesh.

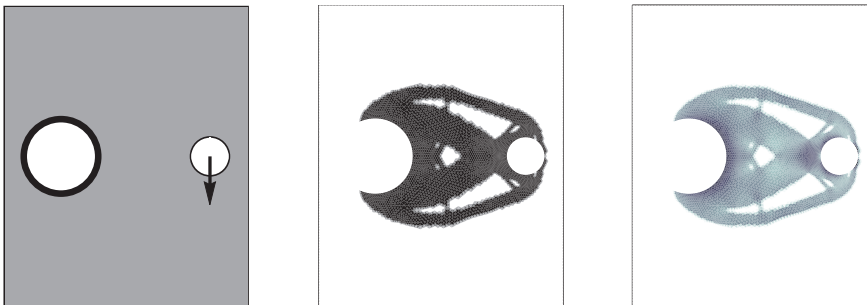


FIGURE 5. Michell's structure: boundary conditions and unconstrained solution with the corresponding Von Mises stress distribution.

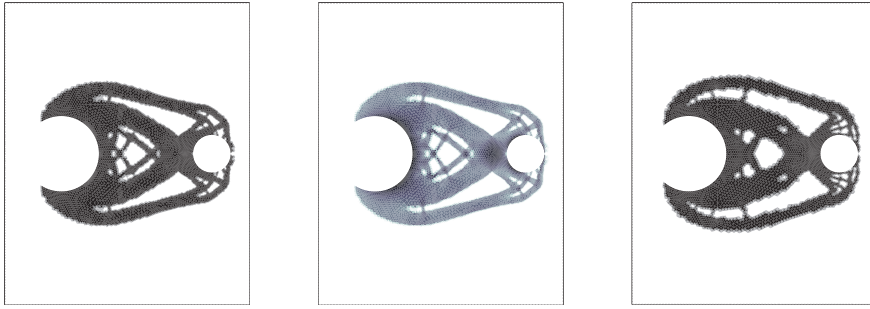


FIGURE 6. Michell's structure: optimal domain for $\alpha = 100$ (left) and Von Mises stress distribution, optimal domain for $\alpha = 500$ (right).

α	β	Area	Compliance	$I_{\Omega}(u_{\Omega})$	$\max_{\Omega} \frac{\sigma_M(u_{\Omega})}{\bar{\sigma}_M}$	CPU time (s)	Mesh
0	0.078	1007	11453	1901	1.68	188	13599
100	0.04	1007	11979	1486	1.02	319	17124
500	0.04	1062	11616	1527	0.97	176	13599

TABLE 2. Michell's structure.

5.3. **Eyebar.** In this example, the working domain is a rectangle of size 16×8 deprived of a circular hole of radius 1.5. On the border of this hole, a horizontal load of density $g(x, y) = ((y^2 - 1.5^2)\chi_{x \leq 0}, 0)$ is applied, where (x, y) denotes a local coordinate system whose origin is at the center of the hole. On the right side, the structure is clamped along a segment of length 2 (see Fig. 7). Here and in the subsequent examples, the subdomain \bar{D} is represented in gray. Again, we show results obtained in the unconstrained ($\alpha = 0$) and constrained ($\alpha = 500$, $\bar{\sigma}_M = 5$) cases, with β adjusted in order to obtain similar areas (see Fig. 7 and Table 3).

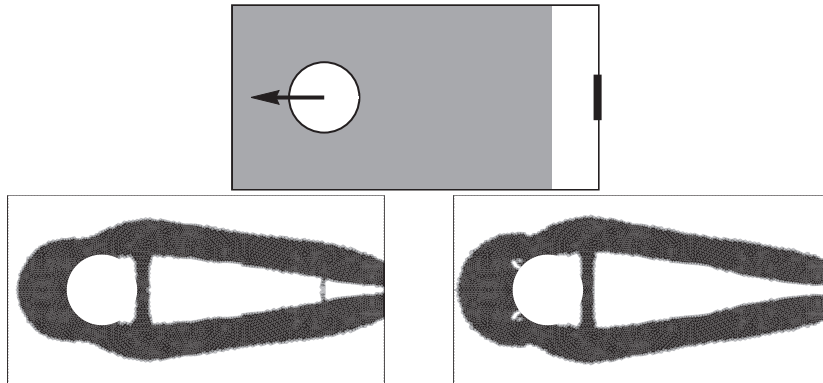


FIGURE 7. Eyebar: boundary conditions and obtained domains for $\alpha = 0$ and $\alpha = 500$.

α	β	Area	Compliance	$\max_{\Omega} \frac{\sigma_M(u_{\Omega})}{\bar{\sigma}_M}$	CPU time (s)	Mesh
0	0.25	46.3	187	1.31	169	13520
500	0.2	46.4	193	0.99	206	13520

TABLE 3. Eyebar.

5.4. **L-beam.** We now turn to a classical problem containing a geometrical singularity, namely the L-shaped beam (see Fig. 8 and 9 and Table 4). The length of the two branches is 2.5. The structure is clamped at the top, and a unitary pointwise force is applied at the middle of the

right tip. We first show a result obtained in the unconstrained case ($\alpha = 0$, $\beta = 0.01$). Then we take the parameters $\alpha = 10^4$, $\beta = 0.01$ and three different values for $\bar{\sigma}_M$: 40, 30 and 25. We observe that, in these last three cases, the reentrant corner is rounded, unlike what occurs in the first case, when minimizing the compliance without stress constraint.

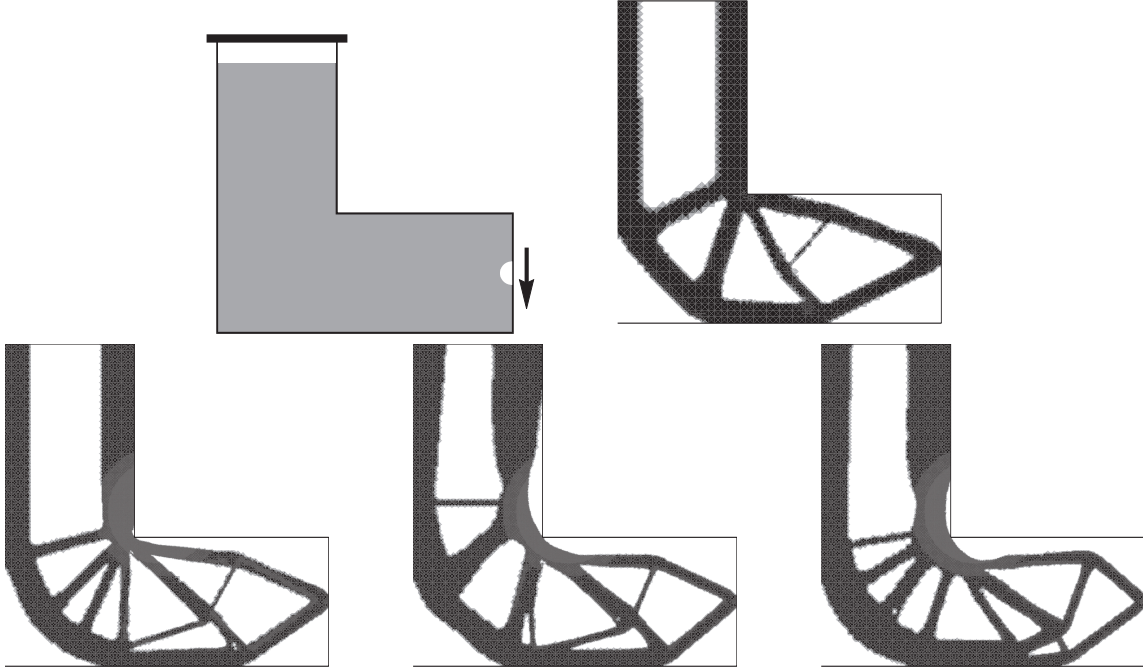


FIGURE 8. L-beam: boundary conditions and obtained design in the unconstrained case (top), obtained designs with the penalization for $\bar{\sigma}_M = 40$, $\bar{\sigma}_M = 30$ and $\bar{\sigma}_M = 25$ (bottom, from left to right).

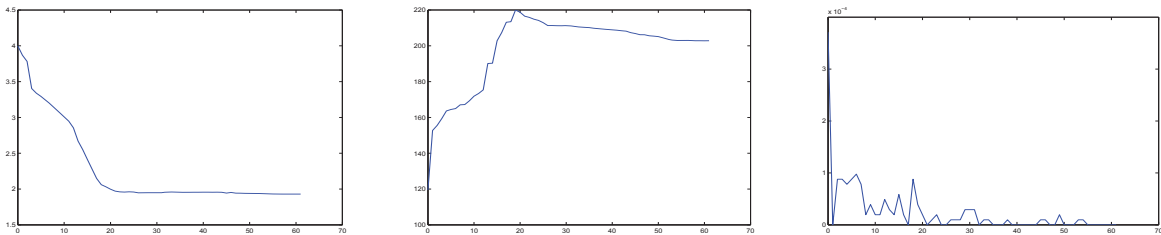


FIGURE 9. L-beam with $\bar{\sigma}_M = 30$: convergence history for the area, the compliance and the area of the region in which the constraint is violated (from left to right).

α	β	$\bar{\sigma}_M$	Area	Compliance	$\max_{\Omega} \frac{\sigma_M(u_{\Omega})}{\bar{\sigma}_M}$	CPU time (s)	Mesh
10^4	10^{-2}	40	1.74	186	1.01	891	26693
10^4	10^{-2}	30	1.93	203	0.99	672	26708
10^4	10^{-2}	25	2.05	181	1.01	536	26678

TABLE 4. L-beam.

5.5. U-beam. This last example consists in an U-shaped structure included in a box of size 3×2.5 (see Fig. 10). We show a result obtained with the parameters $\beta = 0.3$, $\bar{\sigma}_M = 4$ and $\alpha = 10^4$. We get $\max_{\Omega} \frac{\sigma_M(u_{\Omega})}{\bar{\sigma}_M} = 1.02$ on a mesh of 28385 nodes, in 363s of CPU time.

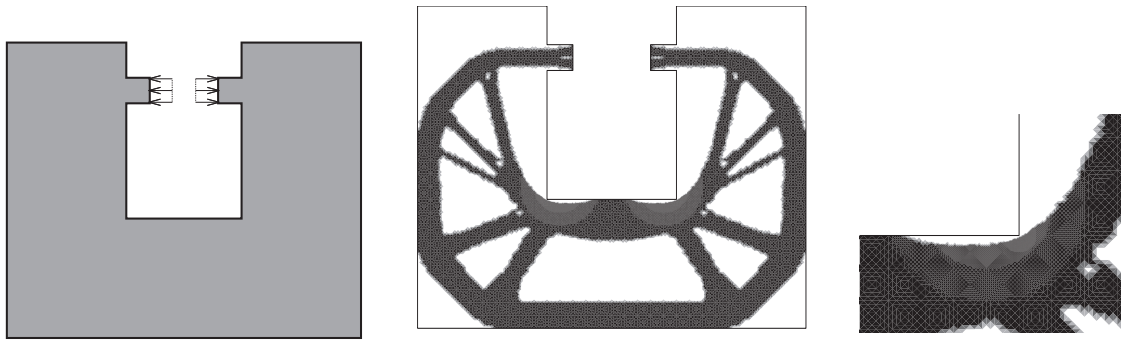


FIGURE 10. U-beam: boundary conditions, obtained design and zoom near a reentrant corner.

5.6. Conclusion. In the above examples, we have minimized a linear combination of the area and the compliance of an elastic structure while prescribing an upper bound on the Von Mises stress at each point. The two basic ingredients of our approach are the use of the topological derivative as a descent direction and of a penalty method for the constraint imposition. This is in contrast with the existing literature on the topic, where either dual methods are implemented [14, 16, 19, 31], with the well-known difficulties related to the irregularity of the Lagrange multiplier, or a simple power law penalization is considered [3, 4], generally leading to unfeasible domains. Furthermore, the topological derivative does not rely on any relaxation, which is a quite delicate issue for local criteria. Finally, the computational cost of this algorithm is remarkably low.

REFERENCES

- [1] G. Allaire. *Shape optimization by the homogenization method*, volume 146 of Applied Mathematical Sciences. Springer-Verlag, New York, 2002.
- [2] G. Allaire. *Conception optimale de structures*, volume 58 of Mathématiques et applications. Springer-Verlag, Berlin, 2007.
- [3] G. Allaire, F. Jouve, & H. Maillot. Topology optimization for minimum stress design with the homogenization method. *Struct. Multidiscip. Optim.* 28(2-3):87-98, 2004.
- [4] G. Allaire & F. Jouve. Minimum stress optimal design with the level-set method. *Eng. Anal. Bound. Elem. special issue*, 32(11):909-918, 2008.
- [5] S. Amstutz, I. Horchani & M. Masmoudi. Crack detection by the topological gradient method. *Control and Cybernetics*, 34(1):81-101, 2005.
- [6] S. Amstutz. Sensitivity analysis with respect to a local perturbation of the material property. *Asymptotic Analysis*, 49(1-2):87-108, 2006.
- [7] S. Amstutz & H. Andrä. A new algorithm for topology optimization using a level-set method. *Journal of Computational Physics*. 216(2):573-588, 2006.
- [8] S. Amstutz. A penalty method for topology optimization subject to a pointwise state constraint. ESAIM:COCV, to appear.
- [9] D. Auroux, M. Masmoudi & L. Belaid. Image restoration and classification by topological asymptotic expansion. *Variational Formulations in Mechanics: Theory and Applications - CIMNE*, Barcelona, Spain 2006.
- [10] M. P. Bendsøe & N. Kikuchi. Generating optimal topologies in structural design using a homogenization method. *Comput. Methods Appl. Mech. Engrg.*, 71(2):197-224, 1988.
- [11] M. P. Bendsøe & O. Sigmund. *Topology optimization. Theory, methods and applications*. Springer-Verlag, Berlin, 2003.
- [12] M. Bonnet. Topological sensitivity for 3D elastodynamic and acoustic inverse scattering in the time domain. *Comp. Meth. in Appl. Mech. Engrg.* 195:5239-5254, 2006.
- [13] M. Burger, B. Hackl & W. Ring. Incorporating topological derivatives into level set methods. *Journal of Computational Physics*, 1(194):344-362, 2004.
- [14] M. Burger & R. Stainko. Phase-field relaxation of topology optimization with local stress constraints. *SIAM J. Control Optim* 45(4):1447-1466, 2006.
- [15] J. Cea, S. Garreau, Ph. Guillaume & M. Masmoudi. The shape and Topological Optimizations Connection. *Computer Methods in Applied Mechanics and Engineering*, 188(4):713-726, 2000.

- [16] P. Duysinx & M. P. Bendsøe. Topology optimization of continuum structures with local stress constraints. *International Journal for Numerical Methods in Engineering*, (43):1453–1478, 1998.
- [17] H.A. Eschenauer & N. Olhoff. Topology Optimization of Continuum Structures: A Review. *Applied Mechanics Review*, **54**:331–390, 2001.
- [18] H.A. Eschenauer, V.V. Kobolev & A. Schumacher. Bubble Method for Topology and Shape Optimization of Structures, *Structural Optimization*, 8:42-51, 1994.
- [19] E.A. Fancello. Topology optimization for minimum mass design considering local failure constraints and contact boundary conditions. *Structural and Multidisciplinary Optimization*, 32(3):229-240, 2006.
- [20] G.R. Feijóo. A new method in inverse scattering based on the topological derivative. *Inverse Problems*, 20(6):1819-1840, 2004.
- [21] S. Garreau, P. Guillaume & M. Masmoudi. The topological asymptotic for PDE systems: the elasticity case. *SIAM J. Control Optim.* 39(6):1756:1778, 2001.
- [22] P. Grisvard. Singularités en élasticité. *Arch. Rational Mech. Anal.* 107(2):157-180, 1989.
- [23] A. Henrot & M. Pierre. *Variation et optimisation de formes*. Volume 48 of Mathématiques et applications, Springer-Verlag, Heidelberg, 2005.
- [24] M. Hintermüller. Fast level set based algorithms using shape and topological sensitivity. *Control and Cybernetics*, 34(1):305–324, 2005.
- [25] L. Jaafar Belaid, M. Jaoua, M. Masmoudi & L. Siala. Application of the topological gradient to image restoration and edge detection. *Eng. Anal. Bound. Elem. special issue*, 32(11):891-899, 2008.
- [26] I. Larrabide, R.A. Feijóo, A.A. Novotny & E. Taroco. Topological Derivative: A Tool for Image Processing. *Computers & Structures* 36(13-14):1386-1403, 2008.
- [27] D. Knees, A.-M. Sändig. Regularity of elastic fields in composites. Multifield problems in solid and fluid mechanics, 331–360, Lect. Notes Appl. Comput. Mech., 28, Springer, Berlin, 2006.
- [28] S. Lee & B.M. Kwak. Smooth boundary topology optimization for eigenvalue performance and its application to the design of a flexural stage. *Engineering Optimization*, 40(3):271-285, 2008.
- [29] M. Masmoudi, J. Pommier & B. Samet. The topological asymptotic expansion for the Maxwell equations and some applications. *Inverse Problems*. 21:547-564, 2005.
- [30] S. A. Nazarov & J. Sokolowski. Asymptotic analysis of shape functionals. *Journal de Mathématiques Pures et Appliquées*. 82(2):125-196, 2003.
- [31] J.T. Pereira, E.A. Fancello & C.S. Barcellos. Topology optimization of continuum structures with material failure constraints. *Structural and Multidisciplinary Optimization*, 26(1,2):50-66, 2004.
- [32] G.N. Savin. *Stress concentration around holes*. V.1. Pergamon Press, New York-Oxford-London-Paris, 1961.
- [33] J. Sokolowski & A. Zochowski. On the Topological Derivatives in Shape Optmization. *SIAM Journal on Control and Optimization*. 37(4):1251-1272, 1999.

(S. Amstutz) LABORATOIRE D'ANALYSE NON LINÉAIRE ET GÉOMÉTRIE, FACULTÉ DES SCIENCES, 33 RUE LOUIS PASTEUR, 84000 AVIGNON, FRANCE.

E-mail address: samuel.amstutz@univ-avignon.fr

(A.A. Novotny) LABORATÓRIO NACIONAL DE COMPUTAÇÃO CIENTÍFICA LNCC/MCT, COORDENAÇÃO DE MATEMÁTICA APLICADA E COMPUTACIONAL, AV. GETÚLIO VARGAS 333, 25651-075 PETRÓPOLIS - RJ, BRASIL.

E-mail address: novotny@lncc.br